

Photodeoxygenation of Dibenzothiophene S-Oxide Derivatives in Aqueous Media

James Korang, Whitney R. Grither, and Ryan D. McCulla*

Department of Chemistry, Saint Louis University, 3501 Laclede Avenue,
Saint Louis, Missouri 63103

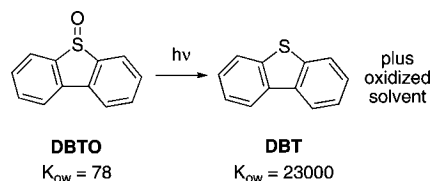
Received January 7, 2010; E-mail: rmccull2@slu.edu

Abstract: The use of atomic oxygen ($O(^3P)$) as potent oxidant in water has suffered from the lack of a facile, efficient source. The photodeoxygenation of aromatic sulfoxides to the corresponding sulfides in organic solvents has been suggested to produce $O(^3P)$ in low quantum yields. The photolysis of 4,6-dihydroxymethylidibenzothiophene S-oxide and 2,8-dihydroxymethylidibenzothiophene S-oxide in water results in deoxygenation at significantly higher quantum yields than in organic solvents. Depending upon conditions, a variable amount of oxidation of the hydroxymethyl substituent into an aldehyde was observed to accompany deoxygenation. Analysis of the photoproducts indicated the deoxygenation occurred by at least two different pH-sensitive mechanisms. Under basic conditions, photoinduced electron transfer yielding a hydroxysulfuranyl radical that decomposed by heterolytic S–O cleavage was thermodynamically feasible. The thermodynamics of photoinduced electron transfer were expected to become increasingly unfavorable as the pH of the solution decreased. Thus, at neutral and acidic pH, an S–O bond scission mechanism was suspected. The observed increase in the photodeoxygenation quantum yields was consistent with charge separation accompanying S–O bond scission. Oxidative cleavage of alkenes in aerobic conditions suggested $O(^3P)$ was produced during photolysis in these conditions; however, the formation of discrete $O^{\cdot-}/HO^{\cdot}$ may occur, particularly at low pH.

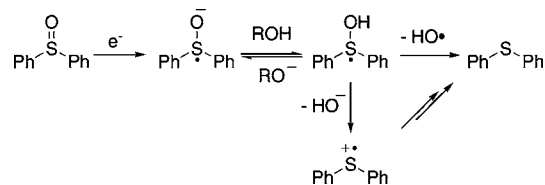
I. Introduction

The earliest suggested pathway for the photoinduced reduction of diaryl sulfoxides invoked the formation of a sulfoxide dimer that ultimately dissociated to singlet or ground-state molecular oxygen and the corresponding sulfides.^{1,2} More recently, an increasing amount of evidence has implicated a unimolecular mechanism for the photodeoxygenation of dibenzothiophene S-oxide (DBTO) and other similar heterocycles.^{3–10} Typically, the observed products of photolysis were dibenzothiophene (DBT) and oxidized solvent as shown in Scheme 1. The oxidant was tentatively assigned as atomic oxygen ($O(^3P)$), or a similar noncovalently bound complex, which was presumably produced by simple scission of the sulfoxide bond.⁵ Additional support for this assertion was obtained by comparing the oxidation of acceptor molecules by $O(^3P)$ in the gas phase and by the photodeoxygenation of DBTO in solution.⁹ This study found the gas- and condensed-phase oxidations have remarkably similar linear relationships between their respective logarithmic

Scheme 1



Scheme 2



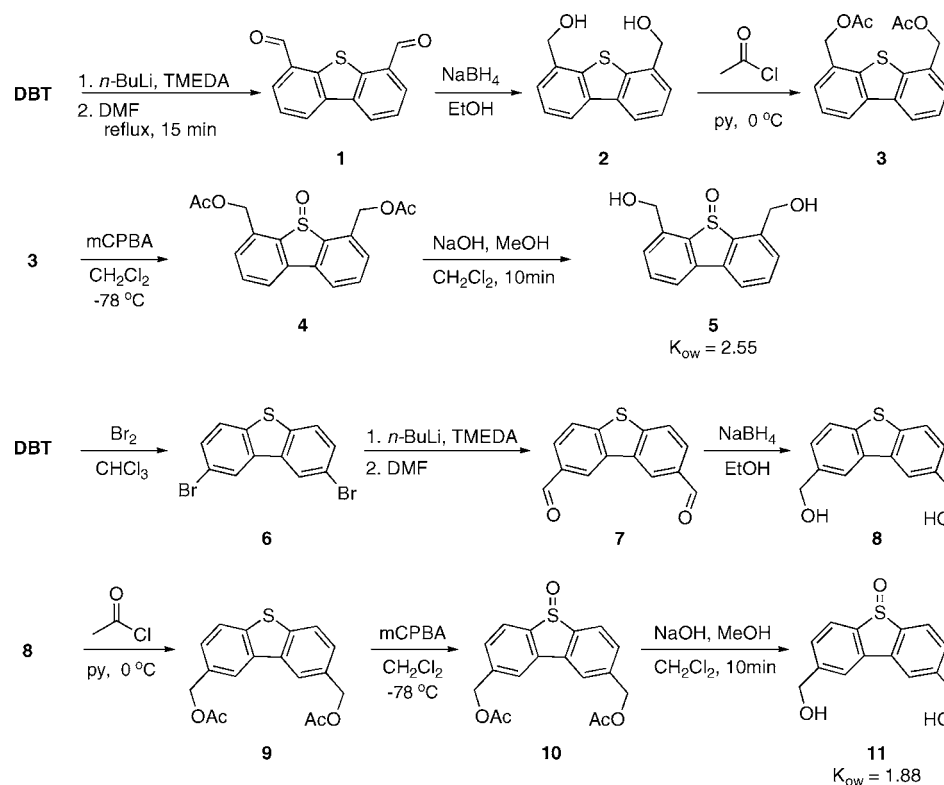
relative rates and ionization potentials of the acceptor molecules, which indicated a similar oxidant.

In alkoxide/alcohol solvent systems, a dramatic increase in the yield of sulfide was observed during the photodeoxygenation of certain sulfoxides.^{11,12} Initiation of the photoreaction by classic electron-transfer agents suggested the formation of a 9-*H*-3-hydroxysulfuranyl radical in one or two steps. The initial electron transfer was most likely a singlet-based process.

- (1) Gurria, G.; Posner, G. *J. Org. Chem.* **1973**, *38* (13), 2419–2420.
- (2) Shelton, J. R.; Davis, K. E. *Int. J. Sulfur Chem.* **1973**, *8* (2), 217–228.
- (3) McCulla, R. D.; Jenks, W. S. *J. Am. Chem. Soc.* **2004**, *126* (49), 16058–16065.
- (4) Wan, Z.; Jenks, W. S. *J. Am. Chem. Soc.* **1995**, *117* (9), 2667–2668.
- (5) Gregory, D. D.; Wan, Z. H.; Jenks, W. S. *J. Am. Chem. Soc.* **1997**, *119* (1), 94–102.
- (6) Nag, M.; Jenks, W. S. *J. Org. Chem.* **2004**, *69* (24), 8177–82.
- (7) Nag, M.; Jenks, W. S. *J. Org. Chem.* **2005**, *70* (9), 3458–63.
- (8) Thomas, K. B.; Greer, A. *J. Org. Chem.* **2003**, *68* (5), 1886–91.
- (9) Lucien, E.; Greer, A. *J. Org. Chem.* **2001**, *66* (13), 4576–9.
- (10) Rockafellow, E. M.; McCulla, R. D.; Jenks, W. S. *J. Photochem. Photobiol. A* **2008**, *198* (1), 45–51.

- (11) Kropp, P.; Fryxell, G.; Tubergen, M.; Hager, M.; Harris, G., Jr.; McDermott, T., Jr.; Tornero-Velez, R. *J. Am. Chem. Soc.* **1991**, *113* (19), 7300–7310.
- (12) Cabbage, J. W.; Tetzlaff, T. A.; Groundwater, H.; McCulla, R. D.; Nag, M.; Jenks, W. S. *J. Org. Chem.* **2001**, *66* (25), 8621–8628.

Scheme 3



Dependent upon the solvent conditions, heterolytic and homolytic cleavage of the sulfur–oxygen bond of hydroxysulfuranyl radicals has been observed, as shown in Scheme 2. Solvent isotope effects indicated the hydroxysulfuranyl radical dissociated by heterolytic cleavage of the S–O bond in methanol; however, homolytic bond scission could not be completely ruled out.

In aqueous solutions, the potent oxidation of solute molecules by O(³P) is expected since the reaction between water and O(³P) to form two HO• is 18 kcal/mol endergonic.^{13,14} The gas-phase reactivity of O(³P) is significantly different than other reactive oxygen species, and if this trend continues in the aqueous media, distinct O(³P) oxidation products are expected in aqueous media.^{15–18} In addition to other reactive oxygen species, such as HO[•]/O^{•-}, small yields of O(³P) have been observed during the photolysis of oxoanions in aqueous solution.^{19,20} Despite the prospect of potent O(³P)-mediated reactions leading to oxidation products distinct from other ROS, the absence of an efficient source has limited the potential use of O(³P) in water.

Additionally, the formation of O(³P) has been implicated in various active oxygen processes; however, the absence of a practical means of independent generation confirming the involvement of O(³P) was difficult.^{21,22} Recently, O(³P)-

mediated cleavage of DNA was demonstrated, which raises the interesting potential use of O(³P) in biological systems.²³ In this work, we report the formation of an oxidant with characteristics consistent with O(³P) during the photolysis of DBTO derivatives in acidic and neutral water.

II. Results

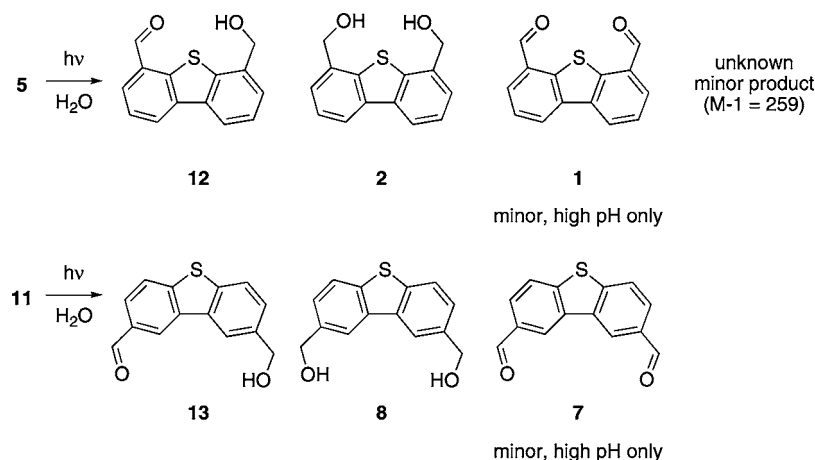
Dibenzothiophene S-oxide (DBTO, *K*_{ow} = 78)²⁴ and dibenzothiophene (DBT, *K*_{ow} = 2.3 × 10⁴)²⁵ are both insoluble in water, which complicates the investigation of their photochemistry in aqueous media. To improve the aqueous solubility of DBTO, 4,6-dihydroxymethyldibenzothiophene S-oxide (**5**) and 2,8-dihydroxymethyldibenzothiophene S-oxide (**11**) were synthesized from DBT as shown in Scheme 3. The octanol–water coefficients (*K*_{ow}) of **5** and **11** were measured to be 2.55 and 1.88, respectively. Thus, **5** and **11** are approximately 40 times more hydrophilic than DBTO. Sufficient quantities of **5** and **11** could be dissolved in water to achieve concentrations between 1.5 and 3.0 mM depending on the pH. The maximum concentration attained was 3.0 mM of **11** at pH 12. No concentration dependence was observed for the UV spectrum of **5** or **11** (Figures S1 and S2 in the Supporting Information).

Photoproducts of 5 and 11. To determine if the photoreduction of aromatic sulfoxides occurs in aqueous media, solutions containing the sulfoxides **5** or **11** were irradiated by broadly emitting fluorescent bulbs centered at 350 nm. Unless noted otherwise, all solutions were purged of oxygen by bubbling argon (>15 min) before photolysis. For unbuffered solutions,

(13) Koppenol, W.; Liebman, J. *J. Phys. Chem.* **1984**, *88* (1), 99–101.
 (14) Braunstein, M.; Panfili, R.; Shroll, R.; Bernstein, L. *J. Chem. Phys.* **2005**, *122* (18), 184307.
 (15) Herron, J.; Huie, R. *J. Phys. Chem. Ref. Data* **1974**, *2* (3), 467–518.
 (16) Kennedy, R.; Mayhew, C.; Peverall, R.; Watts, P. *Phys. Chem. Chem. Phys.* **2000**, *2* (14), 3145–3153.
 (17) Atkinson, R. *Chem. Rev.* **1985**, *85* (1), 69–201.
 (18) Murray, R.; Kaplan, M. *J. Am. Chem. Soc.* **1968**, *90* (15), 4161–4162.
 (19) Warneck, P.; Wurzing, C. *J. Phys. Chem.* **1988**, *92*, 6278–6283.
 (20) Klänig, U.; Sehested, K.; Wolff, T. *J. Chem. Soc., Faraday Trans. 1* **1984**, *80* (11), 2969–2979.
 (21) Tang, X.; Weavers, L. K. *J. Photochem. Photobiol. A* **2007**, *187* (2–3), 311–318.

(22) Tseng, Y.; Kuo, C.; Huang, C.; Li, Y.; Chou, P.; Cheng, C.; Wong, M. *Nanotechnology* **2006**, *17* (10), 2490–2497.
 (23) Wauchope, O. R.; Shakya, S.; Sawwan, N.; Liebman, J. F.; Greer, A. *J. Sulfur Chem.* **2007**, *28* (1), 11–16.
 (24) Octanol–water coefficient from this work.
 (25) Andersson, J.; Schrader, W. *Anal. Chem.* **1999**, *71* (16), 3610–3614.

Scheme 4



the pH was varied by adding either dilute H_2SO_4 or NaOH . Photolysis reactions were also carried out in 0.1 M sodium acetate (pH = 3.6) and 0.1 M glycine– NaOH (pH = 10.6)-buffered solutions. When the photolyses of **5** and **11** were carried out to low conversion (<10%) at neutral or acidic pH, substantial amounts of two photoproducts were detected by HPLC analysis of the photolysis mixture. For **5**, in addition to the two major photoproducts, a minor photoproduct was also detected in acidic and neutral solutions. When the photolysis was run at high pH, a previously unobserved minor product was detected in addition to the other photoproducts for both **5** and **11**. At longer irradiation times, trace amounts (<1%) of other possible photoproducts were also observed.

The corresponding sulfides of **5** and **11**, 4,6-dihydroxymethylidibenzothiophene (**2**) and 2,8-dihydroxymethylidibenzothiophene (**8**), respectively, were expected photoproducts. The sulfides were confirmed as one of the predominant photoproducts by HPLC comparison to authentic samples. However, the sulfide was not the major photoproduct in many of the photolysis conditions. To isolate the other major photoproduct, samples of basic water saturated with either **5** or **11** were irradiated at 330 nm. The unknown product was extracted and purified by preparative TLC before characterization by MS, ^1H NMR, IR (Supporting Information). Due to the limit of the solubility of **5** and **11**, acquiring large amounts of the unknown products was difficult. For both **5** and **11**, GC–MS analysis of the unknown major photoproduct revealed a m/z 242 molecular ion peak. The ^1H NMR spectra of the unknown photoproducts revealed six nonequivalent aromatic, one aldehyde, and two diastereotopic benzylic protons by analysis of the signals' chemical shift. The IR spectra of both unknown photoproducts had a broad peak centered around 3300 cm^{-1} and a weaker peak near 2700 cm^{-1} . Additionally, the unknowns both displayed a strong signal near 1685 cm^{-1} . Therefore, 4-formyl-6-hydroxymethylidibenzothiophene (**12**) and 2-formyl-8-hydroxymethylidibenzothiophene (**13**) were assigned as the other dominant photoproducts of **5** and **11**, respectively. The diformylsulfide analogues of **2** and **8** (i.e., 4,6-diformyldibenzothiophene (**1**) and 2,8-diformyldibenzothiophene (**7**), respectively) were identified by HPLC comparison to authentic samples as the minor products only observed at high pH. Isolation of the minor photoproduct specific to **5** could not be achieved due to the low yield and limited solubility of **5**. However, ESI-MS revealed the unknown minor product specific to **5** gave rise to a $m/z = 259$ ($M - 1$) ion in negative-ion mode. The identified photoproducts are illustrated in Scheme 4.

Table 1. Yields of Photoproducts from the Photolysis of **5** and **11** in Different Conditions^a

sulfoxide	pH	% sulfide ^b	% formyl sulfide ^c	% diformyl sulfide ^d
5	2.8 ^{f,g}	15.7	55.7	2.9
	3.6 ^{e,g}	17.1	62.9	1.4
	6.2 ^{f,g}	12.4	76.4	1.0
	7.0 ^{f,h}	17.5	72.5	– ⁱ
	12.0 ^{f,h}	3.9	89.4	6.7
	12.8 ^{f,g}	4.7	74.5	16.0
11	3.6 ^{e,g}	46.2	46.2	–
	4.1 ^{f,g}	39.1	43.8	–
	7.0 ^{f,g}	44.6	42.9	–
	7.0 ^{f,h}	51.5	33.5	–
	10.6 ^{f,g,j}	32.1	50.3	–
	11.2 ^{f,g}	15.2	66.8	11.7

^a Percent yields in relation to loss of the starting sulfoxide after >90% conversion, unless noted otherwise. ^b **2** for **5** and **8** for **11**. ^c **12** for **5** and **13** for **11**. ^d **1** for **5** and **7** for **11**. ^e Buffered solution. ^f Unbuffered solution. ^g Argon sparged. ^h Purged of oxygen by freeze–pump–thaw cycles. ⁱ Not detected. ^j Percent yields at 25% conversion.

When carried out to >90% conversion, the major product of the photolysis was dependent upon the pH of the solution as shown Table 1. At every condition examined, the major photoproduct observed during the photolysis of **5** was **12**. For **11**, similar amounts of **8** and **13** were observed at pH values between 2 and 8; however, the major product was **13** at high pH. Oxidation of both hydroxymethyl substituents was only significant at high pH. For both **5** and **11**, the ratio of the photoproducts remained approximately the same at acidic and neutral pH. For the irradiation of **11** at pH 11.2 with 330 nm light, a plot of the formation of the photoproducts versus time is shown in Figure 1. Analysis of this plot revealed an induction period associated with formation of diformylsulfide **7**, which indicated **7** was a secondary photoproduct. This assessment was also supported by control experiments that showed the formation of **12** and **13** were observed when **2** and **8**, respectively, were irradiated in basic solutions. At acidic and neutral pH, **2** and **8** were essentially photostable; however, at very long photolysis times (>18 h), trace amounts of **12** and **13** were observed at neutral pH. Additional experiments revealed that **2**, **5**, **8**, and **11** were all stable at 37 °C in the dark throughout the range of pH values used in this study. There were no significant changes in the pH over the course of any of the photolysis reactions.

Quantum Yields. It has been previously observed that the quantum yield of the electrophilic oxidant associated with the photodeoxygenation of DBTO in organic solvent increases at

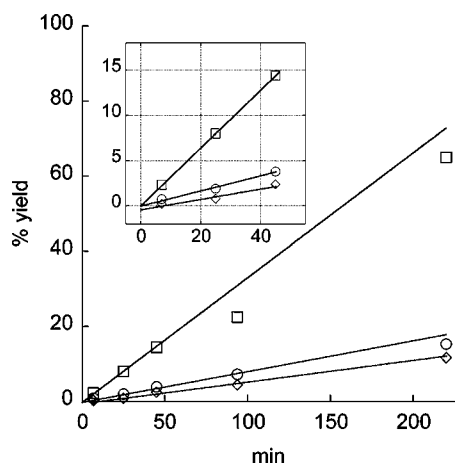


Figure 1. Yields of **7** (diamonds), **8** (circles), and **13** (squares) over time from the photolysis of an aqueous solution of **11** (2.1 mM) at pH = 12. Lines are extrapolations of the linear regression fits of the yields from the first three time points. Inset is an expansion of the data for the first three time points. The y-intercepts for **8** and **13** are near zero, and the y-intercept for **7** is -0.3% .

shorter wavelengths.⁵ To determine if the efficiency of photodeoxygenation was wavelength-dependent, quantum yields for the disappearance of sulfoxides **5** and **11** and the appearance of the corresponding primary photoproducts were determined at 254, 294, and 330 nm, as shown in Table 2. Monochromatic light was generated by focusing a 75 W Xe arc lamp through a monochromator, and the slits were adjusted to a total linear dispersity of 12 nm. The photon flux was determined using azoxybenzene as an actinometer.²⁶ The starting concentrations of **5** and **11** were set to reach an optical density of slightly greater than 2 at the irradiating wavelength. Thus, the starting concentrations ranged between 0.5 and 2.5 mM, with concentrations for irradiations at 254 nm on the low end and 330 nm on the high end. All quantum yield measurements were carried out to less than 25% conversion of the starting sulfoxide. Quantum yields were determined at acidic, neutral, and basic pH, and there was no significant difference observed in the quantum yields for the buffered solutions. However, a substantial increase in the quantum yields was observed in 0.2 M NaCl solutions. Photolysis of **5** (1.7 mM) at high pH resulted in the rapid formation of a precipitate, which interfered with the determination of the quantum yields at 294 and 330 nm.

The observed quantum yields were dependent upon the pH of the photolysis mixture. Usually, the quantum yields for the deoxygenation of the sulfoxides were slightly less than 0.1. Typically, the quantum yields at neutral pH were slightly less than those observed at low and high pH values. As expected from the complete photolysis experiments, quantum yields for the formation of formyl sulfides **12** and **13** increased at high pH at the expense of sulfides **2** and **8**, respectively. Also, as with complete conversion, the ratio of Φ_{+2}/Φ_{+12} and Φ_{+8}/Φ_{+13} was roughly similar in acidic and neutral conditions; however, in most cases, an increase in the amount of the corresponding sulfides (i.e., **2** and **8**) was observed at low pH.

Mechanistic Studies. To provide insight into whether the photoproducts were formed by a unimolecular or bimolecular mechanism, the photolysis of sulfoxide **11** was repeated at 77 K in EPA glass at low concentrations (25 μM). All samples

were sparged with argon and immediately quick-frozen by immersion into liquid nitrogen. The hydroxylic solvent mixture and the low concentration were expected to limit the amount of aggregation of **11** in the glass. On the time scale of an excited state, the amount of diffusion at 77 K after absorption of a photon was also certainly insignificant. Under the initial conditions, **11** does not intensely display photoluminescence, but control experiments showed that **8** has a strong signal under similar conditions. After 60 min of photolysis at 254 nm, the samples showed a marked increase in signal strength corresponding to the fluorescence spectra of **8**, as shown in Figure 2. After melting, the samples were then subjected to HPLC analysis, which revealed sulfide **8** as the only photoproduct under these conditions. To determine if formyl sulfide **13** was formed but undetectable due to the low concentration, the experiment was repeated at higher concentrations of **11** (0.2 mM). Again, no **13** was detected. Interestingly, when the experiment was repeated for sulfoxide **5**, sulfide **2** (80%) and formylsulfide **12** (20%) were both observed to form.

Clearly, the EPA matrix is significantly different than an aqueous environment. Thus, the unimolecular photodeoxygenation observed in the matrix does not preclude the possibility of a bimolecular mechanism in water. To access the possibility that photodeoxygenation in water occurred through the formation of a sulfoxide exciplex, sulfoxide **11** (1 mM) was photolyzed in the presence of excess 3-(methylsulfinyl)benzoic acid (**14**, 4 mM) at 330 nm. At this wavelength, only **11** was expected to absorb the incident light. Assuming the excited state of **11** has no preference for associating with itself, loss of oxygen from **14** to form 3-(methylthio)benzoic acid (**15**) would be expected if a sulfoxide dimer were responsible for the deoxygenation. The photolysis reaction was run to completion, and at no time was **15** observed by HPLC analysis. In a control experiment, **15** was stable during the photolysis of **11** in similar conditions.

The photoreduction in alcoholic/alkoxide solvents systems was examined by irradiating solutions of sulfoxide **11** (1.4 mM) with CH_3ONa (100 mM) in methanol. The irradiations were carried out at 330 nm under anaerobic conditions, and the yields were determined by HPLC. The major photoproduct was sulfide **8** (85.3%), and formyl sulfide **13** (26.5%) formed as a minor product. The observed quantum yield for the loss of **11** was 0.13, which was consistent with the photoreduction of diphenyl sulfoxide in similar conditions.¹² Experiments without methoxide also resulted in the formation of **8** and **13** in yields of 17.9% and 14.1%, respectively. Unexpectedly, there were many unknown minor products. Also, the quantum yield for deoxygenation decreased to 0.008.

In a previous study, the photosensitization of diphenyl sulfoxide by 9-methylcarbazole in methanol resulted in the complete conversion of the sulfoxide to the sulfide with high photoefficiency.¹² Since 9-methylcarbazole and **11** both absorb in some capacity at 343 nm, methanolic solutions containing excess 9-methylcarbazole (10 mM) and **11** (0.5 mM) were prepared. The observed quantum yields of sulfide **8** and formylsulfide **13** were 0.012 and 0.0024, respectively. At these concentrations, greater than 98% of the light was absorbed by 9-methylcarbazole when the sample was irradiated at 343 nm (± 2 nm).

To determine if hydroxyl radical ($\text{HO}\cdot$) was potentially the oxidant responsible for the observed photoproducts, sulfides **2** and **8** were exposed to $\text{HO}\cdot$ generated by the Fenton reaction. In both anaerobic and aerobic conditions, exposure to a 10-

(26) Bunce, N. J.; LaMarre, J.; Vaish, S. P. *Photochem. Photobiol.* **1984**, *39* (4), 531–533.

Table 2. Quantum Yields of Formation of the Primary Photoproducts and Loss of the Starting Sulfoxide^a

sulfoxide	λ (nm)	pH	$\Phi_{\text{-sulfoxide}}$	$\Phi_{\text{+sulfide}}^b$	$\Phi_{\text{+formylsulfide}}^c$	$\Phi_{\text{+sulfide}}/\Phi_{\text{+formylsulfide}}$
5	254	3	0.100 ± 0.050^d	0.023 ± 0.004	0.058 ± 0.011	0.40
		7	0.093 ± 0.008	0.012 ± 0.003	0.051 ± 0.035	0.24
		12	0.196 ± 0.004	0.011 ± 0.001	0.235 ± 0.049	0.05
	294	3	0.255 ± 0.180	0.041 ± 0.018	0.116 ± 0.059	0.35
		7	0.055 ± 0.016	0.014 ± 0.001	0.064 ± 0.008	0.22
		3	0.145 ± 0.017	0.031 ± 0.003	0.070 ± 0.003	0.44
	330	7	0.075 ± 0.020	0.016 ± 0.003	0.076 ± 0.027	0.21
		7 ^e	0.245 ± 0.049	0.042 ± 0.009	0.192 ± 0.039	0.22
		3	0.065 ± 0.015	0.035 ± 0.016	0.033 ± 0.020	1.06
11	254	7	0.060 ± 0.019	0.012 ± 0.004	0.016 ± 0.010	0.75
		12	0.040 ± 0.010	0.007 ± 0.001	0.030 ± 0.008	0.23
		3	0.106 ± 0.006	0.067 ± 0.003	0.046 ± 0.001	1.46
	294	7	0.039 ± 0.010	0.026 ± 0.010	0.014 ± 0.008	1.86
		12	0.076 ± 0.025	0.013 ± 0.004	0.052 ± 0.008	0.25
		3	0.093 ± 0.024	0.070 ± 0.007	0.040 ± 0.007	1.75
	330	7	0.061 ± 0.001	0.021 ± 0.005	0.016 ± 0.009	1.31
		12	0.076 ± 0.001	0.018 ± 0.004	0.070 ± 0.010	0.26

^a All quantum yields reported are the average of multiple runs with conversion under 25%. ^b 2 for **5**, and 8 for **11**. ^c 12 for **5**, and 13 for **11**. ^d Standard deviation. ^e Photolysis runs in 0.2 M NaCl solutions.

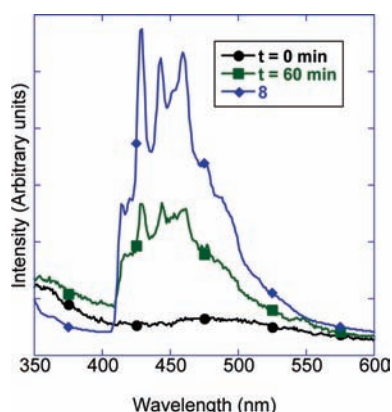


Figure 2. Emission scan of **8** (diamonds) and **11** (25 μM) before (circles) and after (squares) photolysis at 254 nm for 60 min at 77 K.

fold excess of HO \cdot resulted in the conversion of **2** to **12** and **8** to **13** with yields of 10%.

Potentiostatic electrolysis was used to examine the possible fates of radical cations and radical anions formed during photolysis. The electrolysis of sulfide **8** (1 mM) was carried out at 0.8 V vs SCE with 100 mM tetrabutylammonium bromide (TBAB) as the supporting electrolyte. A flow of dry argon into the solution was maintained to limit the amount of oxygen absorbed into the system. The electrolysis was monitored by HPLC, and at the end of the electrolysis a small amount of formyl sulfide **13** was observed in the solution. Additionally, a substantial amount of a solid deposit had formed on the working electrode. After the solid was dissolved in CH₂Cl₂, HPLC analysis revealed the solid comprised significant amounts of diformyl sulfide **7** and formyl sulfide **13**. Electrolysis at -1.7 V vs SCE resulted in the reduction of **11**. In addition to other products, the reduction resulted in the formation of **8** (33%) and **13** (66%).

Redox potentials were determined by square wave voltammetry to investigate the thermodynamic feasibility of photoinduced electron transfer from hydroxide to sulfoxide **11**. The square wave voltammogram of **11** in acetonitrile with tetrabutylammonium perchlorate (TBAP, 100 mM) as the supporting electrolyte can be found in the Supporting Information (Figure S3), which showed that the reduction potential of **11** was $E^\circ(\mathbf{11}^{\cdot-}) = -1.73$ V vs Ag/Ag⁺. To compare the silver wire reference

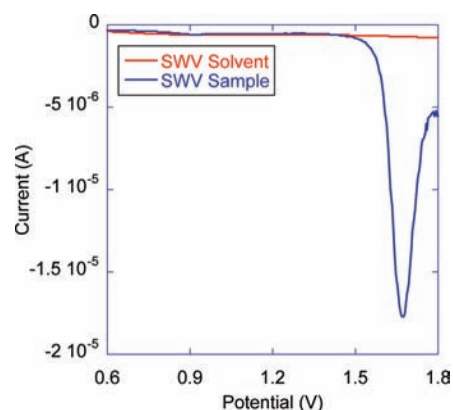


Figure 3. Square wave potential scan of **8** (1 mM) in acetonitrile vs Ag/Ag⁺ with 100 mM of tetrabutylammonium perchlorate (TBAP) as the supporting electrolyte (blue). Square wave potential scan of the same solution immediately prior to the addition of **8** (red).

electrode to NHE, a cyclic voltammogram from 0.0 to 1.5 V vs Ag/Ag⁺ was run on an acetonitrile solution containing ferrocene (10 mM) and TBAP (100 mM). The anodic peak potential was observed at 0.39 V vs Ag/Ag⁺, and the cathodic peak potential was detected at 0.57 V vs Ag/Ag⁺. Using a value of $E^\circ(\text{Fc}^+/\text{Fc})$ 0.31 V vs SCE for the oxidation of ferrocene, the silver wire potential was determined as $E^\circ(\text{Ag}/\text{Ag}^+) = -0.07$ V vs NHE.²⁷ As shown in Figure 3, the square wave voltammogram of sulfide **8** in acetonitrile with 100 mM tetrabutylammonium perchlorate (TBAP) revealed the oxidation potential of **8** was $E^\circ(\mathbf{8}/\mathbf{8}^+) = 1.67$ V vs Ag/Ag⁺. All samples were purged with dry argon immediately before the measurements were made.

In the gas phase, reactions between O(³P) and thiols were some of the most rapid.²⁸ In an attempt to trap O(³P), solutions were prepared containing 3-mercaptopbenzoic acid (**16**, 1.5 mM) and either **5** or **11** (2 mM). All samples were purged of oxygen before irradiation with a narrow band of 330 nm light, and the progress of the photolysis was monitored by HPLC. Quantum

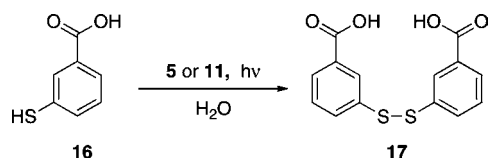
(27) Bard, A. J.; Faulkner, L. R., *Electrochemical Methods: Fundamentals and Applications*, 2nd ed.; John Wiley & Sons, Inc.: Danvers, MA, 2001.

(28) Singleton, D.; Cvetanović, R. *J. Phys. Chem. Ref. Data* **1988**, *17* (4), 1377–1437.

Table 3. Quantum Yields for the Photolysis of **5** and **11** in the Presence of 3-Mercaptobenzoic Acid (**16**)^a

SM	$\Phi_{\text{-sulfoxide}}$	$\Phi_{\text{-16}}$	$\Phi_{\text{+sulfide}}^b$	$\Phi_{\text{+formylsulfide}}^c$	$\Phi_{\text{+17}}$
5	0.13(1) ^d	0.040(7)	0.015(7)	0.12(6)	0.021(8)
11	0.10(1)	0.066(8)	0.036(6)	0.092(11)	0.046(8)

^a All quantum yields reported are the average of multiple runs with conversion under 25%. ^b **2** for **5**, and **8** for **11**. ^c **12** for **5**, and **13** for **11**. ^d Standard deviation indicating uncertainty in the last digit.

Scheme 5**Table 4.** Apparent Quantum Yields for the Photolysis of **5** and **11** in the Presence of Molecular Oxygen^a

SM	$\Phi_{\text{-sulfoxide}}$	$\Phi_{\text{+sulfide}}^b$	$\Phi_{\text{+formylsulfide}}^c$	$\Phi_{\text{+sulfide}}/\Phi_{\text{+formylsulfide}}$
5	0.049	0.0075	0.027	0.27
11	0.027	0.0088	0.010	0.88

^a All quantum yields reported are the average of multiple runs with conversion under 25%. ^b **2** for **5**, and **8** for **11**. ^c **12** for **5**, and **13** for **11**.

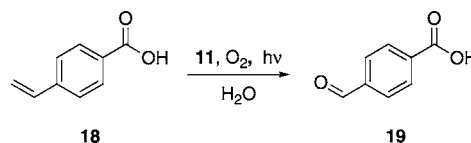
yields for the photoreactions are shown in Table 3. As shown in Scheme 5, one new product was observed and was identified as 3,3'-dithiobisbenzoic acid (**17**), the disulfide of **16**, by comparison to an authentic sample. It was found at low pH that the sulfoxides **5** and **11** were not stable in the presence of **16**, and at high pH, **17** was observed to thermally return to **16**. Thus, the photolysis reactions were run in solutions near a pH of 8. At this pH value, **17** was not observed when solutions containing **16** and **11** were kept in the dark at 37 °C for 19 h. Additionally, direct irradiations of **16** did not result in the formation of **17**. At this pH, no change in the concentration of **17** observed at four times longer than the typical photolysis reaction.

Effect of O₂ on the Photochemistry of 5 and 11. Photolysis of oxoanions in aerated water was shown to form ozone, presumably from a reaction between O(³P) and O₂.²⁰ When the photolysis reactions of sulfoxides **5** and **11** were carried out while bubbling O₂ through the solution, two additional minor products were formed in addition to the products observed in anaerobic conditions (Table 4). Separation of the unknown products by HPLC was complicated by poor separation, and the low yields prevented easy large-scale preparation. To determine if any of the photoproducts arose from singlet oxygen, control experiments with aerated solutions containing methylene blue (0.15 mM), a photosensitizer known to generate singlet oxygen,²⁹ and either **11** or **8** (1.5 mM) were irradiated with fluorescent bulbs fitted with 530 nm long-pass filters. At this wavelength, only methylene blue was expected to absorb the irradiation. None of the photoproducts were observable by HPLC analysis. Besides the addition of 10% of acetonitrile as a cosolvent, benzyl phenyl sulfide was oxidized to the corresponding sulfoxide and sulfone under similar conditions, which was consistent with the previously reported oxidation of benzyl phenyl sulfide by singlet oxygen.³⁰ Also, the photolysis of sulfoxide **11** did not lead to the oxidation of benzyl phenyl

Table 5. Quantum Yields for the Photolysis of **11** in the Presence of 4-Vinylbenzoic Acid (**18**) at 330 nm^a

pH	$\Phi_{\text{-11}}$	$\Phi_{\text{+8}}$	$\Phi_{\text{+13}}$	$\Phi_{\text{+19}}$
3	0.022(3) ^b	0.0044(9)	0.0012(7)	0.0020(4)
7	0.014(1)	0.0019(4)	0.0003(1)	0.0010(6)
12	0.0029(1)	0.0001(1)	0.0014(1)	trace

^a All quantum yields reported are the average of multiple runs with conversion under 25%. ^b Standard deviation indicating uncertainty in the last digit.

Scheme 6

sulfide in the absence of oxygen. Thus, the two unknown photoproducts were unlikely the result of a process involving singlet oxygen.

In a previous study, 4-vinylbenzoic acid (**18**) was unreactive with singlet oxygen; however, **18** reacted with ozone to form 4-formylbenzoic acid (**19**).³¹ Solutions of **18** (5 mM) and **11** (2.0 mM) were prepared and irradiated with monochromatic light (12 nm total linear dispersity) at 330 nm while bubbling oxygen through the solutions. The UV absorption of **18** at high concentrations ended at 310 nm, and thus, sulfoxide **11** was expected to absorb all of the light under these conditions. The quantum yields were measured for the formation products and loss of the sulfoxide, as shown in Table 5. As shown in Scheme 6, the dominant product arising from **18** was **19**. Control experiments found that **18** did not convert to **19** when exposed to singlet oxygen, hydroxyl radicals, or when the samples were kept in the dark for 12 h.

III. Discussion

A significant result from this study was the substantial increase of the quantum yield for the photodeoxygenation of the dibenzothiophene S-oxides chromophore in water compared to organic solvents.⁵ The observed quantum yields were expected for photolysis reactions run in basic conditions since similar quantum yields had been reported for the bimolecular photoreduction of diphenyl sulfoxide.¹² In the absence of an electron donor, the largest quantum yield for the photoreduction of an aromatic sulfoxide was 0.010, which occurred in neat cyclohexene, a known chemical trap for O(³P), during irradiation of DBTO. When rapid reactions between O(³P) and the solvent were not expected, quantum yields for the appearance of DBT decrease to approximately 0.003. The quantum yields for the photodeoxygenation of the sulfoxides **5** and **11** in neutral or acidic water ranged from 0.04 to 0.24. Since the reaction between O(³P) and H₂O is endothermic, the increase in quantum yield cannot be explained by a rapid reaction between O(³P) and water.¹⁴ Thus, the solvent effect for water must have another mechanistic explanation.

The first proposed mechanism for the photoinduced reduction of diaryl sulfoxides implicated the formation of a sulfoxide dimer that decomposed to singlet- or ground-state molecular

(29) Khan, A. U.; Kasha, M. *Proc. Natl. Acad. Sci. U.S.A.* **1979**, *76* (12), 6047–6049.

(30) Clennan, E. L.; Zhou, W.; Chan, J. *J. Org. Chem.* **2002**, *67* (26), 9368–78.

(31) Wentworth, P.; McDunn, J. E.; Wentworth, A. D.; Takeuchi, C.; Nieva, J.; Jones, T.; Bautista, C.; Ruedi, J. M.; Gutierrez, A.; Janda, K. D.; Babor, B. M.; Eschenmoser, A.; Lerner, R. A. *Science* **2002**, *298* (5601), 2195–9.

oxygen and two sulfides.^{1,2} However, a unimolecular mechanism was suggested in more recent studies.^{5–9} Due to the large hydrophobic regions of sulfoxides **5** and **11**, increased aggregation might be expected to occur in water. Though the concentration range was limited, the UV-absorption spectra of **5** and **11** showed no concentration dependence, which suggests that association before absorption of the light was limited.

Most of the results in this work argue against the role of a dimer in the photoinduced deoxygenation of the sulfoxides **5** and **11**. The starting sulfoxides and all of the observed photoproducts appeared to be inert to oxidation by singlet oxygen (¹O₂) generated by using methylene blue as a photosensitizer. Also, no evidence for ¹O₂ was observed when benzyl phenyl sulfide was used as a trap during the photolysis of **11**. The oxidation of the benzoic acid **18** was found to be inert to ¹O₂.³¹ Thus, none of the results observed during this study suggested the involvement of singlet oxygen (¹O₂) as a potential oxidant during the photolysis of **5** and **11** in anaerobic or aerobic conditions. Thus, degradation of a sulfoxide exciplex leading to ¹O₂ and two sulfides was largely ruled out as a major process.

Potentially, degradation of the sulfoxide exciplex could lead to ground-state molecular oxygen and two sulfides. Assuming the excited state of **11** does not selectively associate with itself, the direct irradiation of **11** in the presence of the sulfoxide **14** would be expected to yield a sulfoxide dimer of **11** and **14**. Degradation of this dimer would lead to molecular oxygen and the sulfides **8** and **15**; however, **15** was not observed. Also, over the limited range examined, the quantum yields were largely independent of the starting sulfoxide concentrations. While these results do not completely rule out the possibility of a sulfoxide dimer, the involvement of a sulfoxide dimer along the photochemical pathway to deoxygenation was viewed as unlikely.

The photodeoxygenation of sulfoxide **11** to sulfide **8** while isolated in a matrix indicates that a unimolecular process was possible for sulfoxides **5** and **11**. As expected, the corresponding sulfides were the major photoproducts observed during irradiation of **5** and **11** in the matrix. The formation of formyl sulfide **12**, but not formyl sulfide **13**, during irradiations in the EPA matrix suggested that proximity to the sulfoxide functional group influences the susceptibility of the benzylic carbons to oxidation by a unimolecular mechanism. Clearly, conditions in the matrix were quite different than aqueous solutions, and yet, the extent of oxidation of the hydroxymethyl substituents of **5** and **11** in water was quite unexpected. The change in the product and quantum yields between neutral and basic pH was consistent with two distinct mechanisms being involved in the photodeoxygenation.

Similar photochemical mechanisms for **5** and **11** were expected, and thus for simplicity, the focus of the discussion will be sulfoxide **11**. As shown in Scheme 7, three initial events from the excited state of **11** were considered. The quantum yields reported in this paper at high pH were comparable to those reported for the bimolecular photoreduction of diphenyl sulfoxide in alcohol/alkoxide solvent systems.¹² The bimolecular photoreduction of **11** was expected to begin with an electron transfer from HO[−] to the excited state (**11**^{*}) to form the radical anion (**20**). The photoinduced change in free energy for the electron-transfer from HO[−] to **11**^{*} can be estimated from the Rehm–Weller equation (eq 1). Since HO• has no charge, the energy required to separate an ion pair (*W_d*) was approximated as zero. The excitation energy of **11** (ΔE_{00}) was approximated as 3.75 eV. Using 1.77 V vs NHE for $E^\circ(\text{HO}\bullet/\text{HO}^-)$ and -1.80 V vs NHE for $E^\circ(\mathbf{11}/\mathbf{11}^{\bullet-})$, the change in

free energy associated with electron transfer from HO[−] to the excited state of **11** (ΔG_{et}) was approximated as -4.1 kcal/mol exergonic.

$$\Delta G_{\text{et}} = 23.06([E^\circ(\text{HO}\bullet/\text{HO}^-) - E^\circ(\mathbf{11}/\mathbf{11}^{\bullet-})] - W_{\text{d}} - \Delta E_{00}) \quad (1)$$

The *pK_a* of (CH₃)₂SOH• was reported as approximately 17, which suggests **20** would be protonated at the examined pH values to form the hydroxysulfuranyl radical **21**.^{32,33} While persistent sulfuranyl radicals have been reported, hydroxysulfuranyl radicals are generally not stable, and their fate in aqueous solutions has consistently been reported as the heterolytic cleavage to form R₂S⁺ and HO[−].^{32–34} Thus, after protonation of **20**, the subsequently formed **21** would be expected to decompose to the radical cation **22** and HO[−].

The oxidation potential of **8** ($E^\circ(\mathbf{8}^+/\mathbf{8})$ 1.60 vs NHE) measured in acetonitrile suggests the radical cation **22** can oxidize water ($E^\circ(\text{O}_2/\text{H}_2\text{O}) = 0.52$ V vs NHE at pH 12).²⁷ Oxidation of water by **22** would be expected to yield sulfide **8**, oxygen, and protons. Since the oxidation of water is a four-electron process, the oxidation of water by the radical cation **22** is expected to be slow; however, the exergonic nature of the reaction is anticipated to drive the reaction. The expected drop in the pH may not have been detected due to the low yield of **8** in basic conditions. If it is assumed that the oxidation of water by **22** leads to **8**, the dominance of **13** at basic conditions presumably arises from a competing kinetic process that is accelerated by HO[−].

Deprotonation of the hydroxy group of radical cation **22**, which would be more prevalent at high pH, could lead to an alkoxy radical. This alkoxy radical intermediate could disproportionate with sulfide **8** to yield the formylsulfide **13** and sulfide **8**. However, this alkoxy radical intermediate would also be expected to undergo a disproportionation reaction with sulfoxide **11** to yield 2-formyl-8-hydroxydibenzothiophene *S*-oxide, which was not detected even when the photolysis was carried out to high conversion. Thus, it seems unlikely that the formation of **13** is due to a bimolecular disproportionation reaction.

A possible explanation for the increased formation of formylsulfide **13** at high pH is that the radical cation **22** could potentially oxidize HO[−] to O^{•−} ($E^\circ(\text{O}^{\bullet-}/\text{HO}^-) = 1.64$ V vs NHE).¹³ Though, it should be pointed out that this process would be slightly endergonic. Exposure of sulfide **8** to HO• generated by the Fenton reaction yielded **13**. Thus, the oxidation of HO[−] to O^{•−} and a proton could lead to the formylsulfide **13** through a reaction between the nascent sulfide **8** and O^{•−}/HO• ($\text{HO}\bullet$ *pK_a* = 11.9).¹³ However, the process would not be expected to go to completion, and the conversion of **8** to **13** by O^{•−} would require an additional oxidant. Thus, thorough removal of molecular oxygen by freeze–pump–thaw cycles would have been expected to decrease the yield of **13**, and yet, the opposite was observed. Also, the oxidation of HO[−] by **22** would become increasingly endergonic as the pH of the solution decreased, and thus, this process would not be expected to occur at neutral pH.

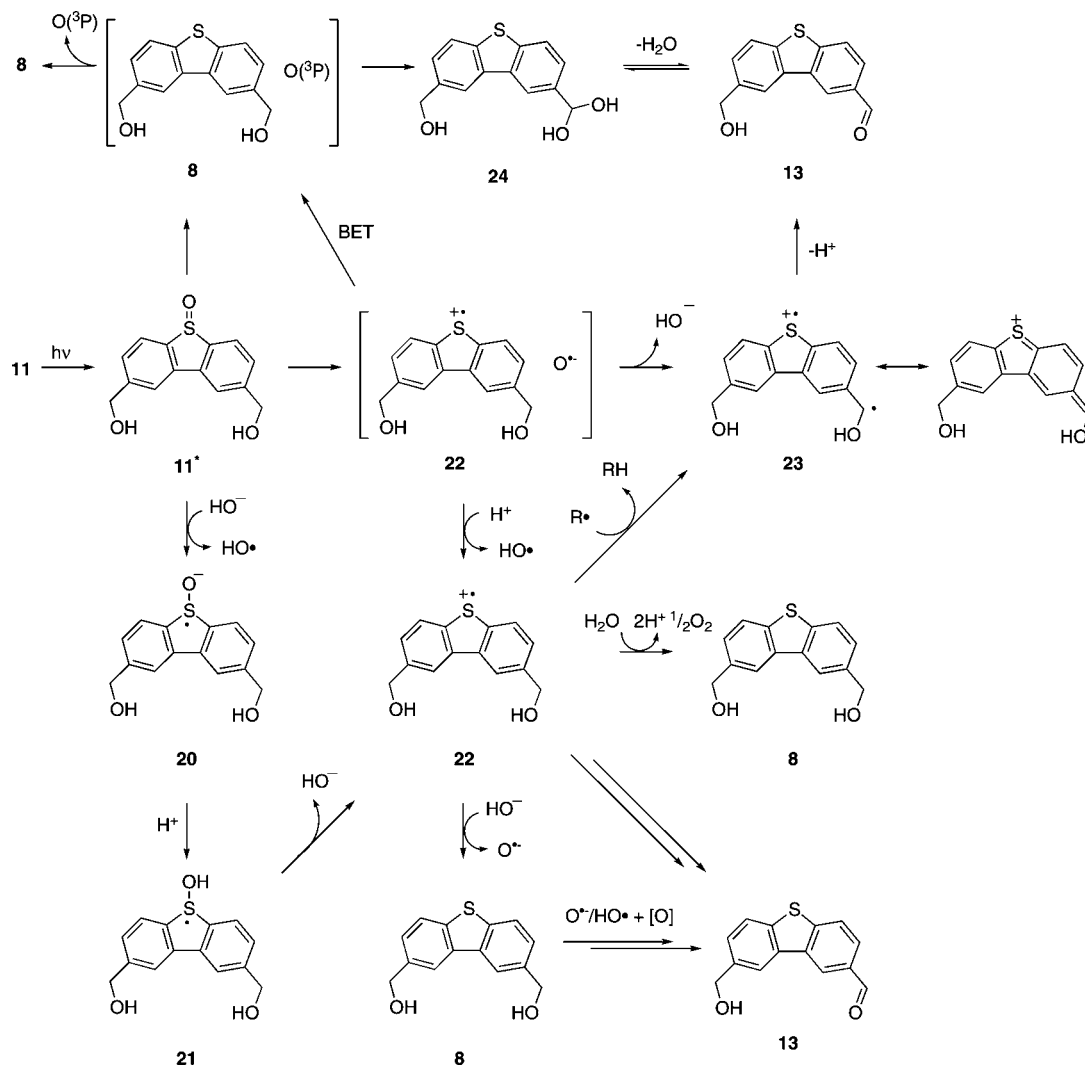
An alternative mechanism to explain the increased formation of formyl sulfide **13** is that the abstraction of a benzylic

(32) Merenyi, G.; Lind, J.; Engman, L. *J. Phys. Chem.* **1996**, *100* (21), 8875–8881.

(33) Chaudhri, S.; Mohan, H.; Anklam, E.; Asmus, K. *J. Chem. Soc., Perkin Trans. 2* **1996**, (3), 383–390.

(34) Perkins, C. W.; Clark, R. B.; Martin, J. C. *J. Am. Chem. Soc.* **1986**, *108*, 3206–3210.

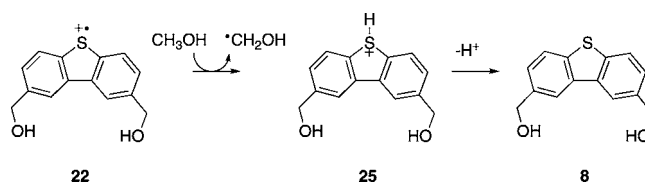
Scheme 7



hydrogen from **22**, or potentially at some step between **20** and **22**, would result in the formation of cation **23**. Deprotonation of the hydroxy functional group of **23** would generate **13**. Certainly, the HO• formed during the reduction of **11*** by HO⁻ could potentially abstract a benzylic hydrogen. Additionally, this mechanism would not effect the pH of the solution. For this proposed pathway, the observed yields of **13** at high pH would necessitate the rate of benzylic hydrogen abstraction being much faster than other potential radical reactions. Thus, this alternative mechanism appears more consistent with the results obtained during this study. However, formation of **13** during the electrolysis of **8** in water at 0.8 V vs SCE suggests other oxidation pathways may also lead to **13**. Thus, other pathways from **22**, or some other intermediate along the bimolecular photoreduction pathway, to **13** may exist or even be dominant at high pH.

In organic solvents, the similar quantum yields in methanol/methoxide and with the electron-donating 9-methylcarbazole suggests that the deoxygenation occurs by photoinduced bimolecular reduction in these conditions. Hydrogen abstraction from the solvent by radical cation **22** yielding the sulfonium **25** has been previously suggested, as shown in Scheme 8.¹² The most probable fate of **25** would be deprotonation yielding sulfide **8**.

Scheme 8



Thus, the increased yield of **8** was consistent with increased formation of **25** in methanol/methoxide solutions compared to basic water.

The proposed photoinduced bimolecular photoreduction is expected to become increasingly unfavorable as the pH of the solution decreases for two reasons. First, the oxidation potential of HO⁻ will increase with a decrease in pH, and thus, the photoinduced electron transfer from HO⁻ to **11*** will become increasingly endergonic. This assessment is supported by the increased yield of sulfide **8** at pH 10.6 where the estimated ΔG_{et} is 0.5 kcal/mol. In acidic conditions (pH 0), $E^\circ(\text{HO}\cdot/\text{H}_2\text{O})$ is 2.59 V vs NHE, and thus, the estimated ΔG_{et} would be 15.0 kcal/mol endergonic.¹³ Second, as written in Scheme 7, the quantum yield for the bimolecular photoreduction of **11** (Φ_{+20}) can be estimated using eq 2. As long as the rate of electron transfer ($k_{[HO^-]}$) is much greater than the sum of all other

unimolecular and pseudounimolecular decay constants ($\sum k_d$), Φ_{+20} would be pH independent. However, assuming k_q is diffusion controlled, the lifetime ($\sum k_d^{-1}$) of **11*** would have to be at least 10 s for the quantum yield to remain unchanged at pH 3. Since the lifetime of DBTO triplet state is 80 ms in a solid matrix, a lifetime of **11*** on the order of seconds is unlikely in solution. Thus, the change of product yields at neutral pH is most likely due to a new photochemical mechanism.

$$\Phi_{+20} = \Phi_I k_q [\text{HO}^-] / (k_q [\text{HO}^-] + \sum k_d) \quad (2)$$

The production of an oxidant with the characteristics of $\text{O}(\text{}^3\text{P})$ during the photodeoxygenation of DBTO led to the suggestion of a simple S–O bond scission.^{5–10} However, the increase in the quantum yield at low and neutral pH is difficult to explain with simple scission of the S–O bond. In organic solvents, the most effective solvents for deoxygenation are nucleophilic traps. However, the reaction between $\text{O}(\text{}^3\text{P})$ and water is endothermic, and thus, it is implausible that a reaction between water and $\text{O}(\text{}^3\text{P})$ increases the quantum yield. An alternative to the simple scission mechanism involves the accompaniment of S–O bond cleavage with charge separation. This process could lead to a discrete contact ion pair consisting of the sulfide radical cation **22** and atomic oxygen anion radicals ($\text{O}^{\cdot-}$) or, alternatively, rapid back electron transfer (BET) would lead to the sulfide **8** and $\text{O}(\text{}^3\text{P})$. A consequent increase in the quantum yield of deoxygenation would be expected with greater solvation of a fleeting or discrete ion pair.

If indeed water helps by stabilizing the ion pair, the possibility arises that discrete atomic oxygen anion radicals ($\text{O}^{\cdot-}$) are formed. The $\text{p}K_a$ of HO^\bullet is 11.9, and thus, persistent $\text{O}^{\cdot-}$ would lead to HO^\bullet in these conditions.³⁵ Once HO^\bullet forms, back-electron transfer would be thermodynamically unfavorable. In addition, protonation of $\text{O}^{\cdot-}$ would limit the ability of radical cation **22** and $\text{O}^{\cdot-}$ to reform sulfoxide **11** in an energy wasting process, which is consistent with the slight increase of overall quantum yields observed at low pH.

If discrete $\text{O}^{\cdot-}$ forms, an explanation for the observed yields of sulfide **8** and formyl sulfide **13** relies on competition between benzylic hydrogen abstraction and the escape of $\text{O}^{\cdot-}/\text{HO}^\bullet$ into the bulk. Abstraction of a benzylic hydrogen from the radical cation **22** by $\text{O}^{\cdot-}$ or HO^\bullet would lead to the cation **23**. Again, deprotonation of the hydroxy functional group would convert **23** into **13**. Escape of $\text{O}^{\cdot-}/\text{HO}^\bullet$ from the solvent cage would allow **22** to oxidize water ($E^\circ(\text{O}_2/\text{H}_2\text{O})$ 1.22 V vs NHE at pH 0) to yield **8**. The increase of $\Phi_{+\text{sulfide}}/\Phi_{+\text{formylsulfide}}$ in Table 2 at low pH can be explained if protonation assists the escape of HO^\bullet from the solvent cage. This is reasonable since the electrostatic attraction between **22** and $\text{O}^{\cdot-}$ would decrease upon protonation. Also, the proximity of the benzylic position to the sulfoxide would be expected to increase the rate of hydrogen abstraction, which is consistent with the degree of oxidation of the benzylic carbons for **5** compared to **11**. Neither benzylic hydrogen abstraction nor protonation from the bulk would be expected to change the pH of the solution. However, if the formation of formylsulfide **13** at high pH is mediated by $\text{O}^{\cdot-}/\text{HO}^\bullet$, the increased yield of sulfide **8** at neutral and acidic pH is inconsistent with the formation of discrete $\text{O}^{\cdot-}$. For consistency, the proposal of discrete $\text{O}^{\cdot-}$ would also require a pathway to **13** without the benzylic hydrogen abstraction by HO^\bullet under basic conditions.

Alternatively, rapid back-electron transfer to form $\text{O}(\text{}^3\text{P})$ and **8** before the formation of discrete **22** and $\text{O}^{\cdot-}$ is also consistent with the increased quantum yields and pH independent product yields. Indirect evidence for the formation of $\text{O}(\text{}^3\text{P})$ during the photodeoxygenation of sulfoxide **11** was gathered by attempting to trap $\text{O}(\text{}^3\text{P})$ with the thiol **16**. It is known that $\text{O}(\text{}^3\text{P})$ reacts with thiols rapidly in the gas phase to form sulfenic acids.²⁸ Sulfenic acids generated by other means in solution react with sulfides to form disulfides.³⁶ The correlation between the formation of **8** and the disulfide **17** suggests the oxidation of **16** was related to the deoxygenation of **11**. In addition to other products, thiols are also converted to disulfides by HO^\bullet , and thus, this result cannot be used to distinguish between the formation of $\text{O}(\text{}^3\text{P})$ and discrete $\text{O}^{\cdot-}$.³⁷

The increased quantum yields in acidic pH compared to neutral solutions suggests the deoxygenation is dependent upon the pH, which would be consistent with the protonation of discrete $\text{O}^{\cdot-}$. However, the increase in the polarity of the solutions through the addition of salts would assist charge separation and concomitantly increase the quantum yields. Indeed, the addition of 0.2 M of NaCl more than doubled the observed quantum yields at neutral pH. The observation that the addition of salt has no effect on the products yields argues against the possibility of a specific salt effect. While certainly possible that the increase in the quantum yields at low pH is due to a greater extent of protonation of $\text{O}^{\cdot-}$, the effect could also be attributed to a general salt effect.

Photolysis reactions that were purged of oxygen by freeze–pump–thaw cycles preclude the possibility that the formation of formylsulfide **13** is dependent upon the presence of molecular oxygen. The insertion of $\text{O}(\text{}^3\text{P})$ into C–H bonds is well-known, and insertion of $\text{O}(\text{}^3\text{P})$ into benzylic C–H bond of **8** would result in the formation of the hydrate of **13** (**24**). Again, a nascent oxidant arising from the sulfoxide would be expected to react faster with the benzylic positions of **5** compared to **11** due to their proximity. Thus, the increased oxidation of benzylic position of **5** supports the supposition of an active oxidant generated from the sulfoxide functional group. Irradiation of DBTO in toluene yields benzyl alcohol and benzaldehyde, in addition to cresols, which indicates benzylic carbons are susceptible to oxidation by $\text{O}(\text{}^3\text{P})$.³ Thus, for a mechanism leading to $\text{O}(\text{}^3\text{P})$ and sulfide **8**, the amount of **8** compared to **13** would be dependent upon the rate at which $\text{O}(\text{}^3\text{P})$ escapes the solvent cage.

The rate constant for the reaction between O_2 and $\text{O}(\text{}^3\text{P})$ to form O_3 has been reported as $4.2 \times 10^9 \text{ M}^{-1} \text{ s}^{-1}$.^{20,38} Consistent with previous reports, conversion of 4-vinylbenzoic acid (**18**) to the 4-formylbenzoic acid (**19**) suggests O_3 was formed during the irradiation of **11** at neutral and acidic pH. However, **18** was inert during the photolysis of **11** in basic conditions, which was expected since the proposed bimolecular photoreduction mechanism does not produce $\text{O}(\text{}^3\text{P})$. This also provides further evidence that the mechanism of photodeoxygenation is different at high and low pH. Additionally, the formation of benzaldehyde during the irradiation of DBTO in styrene supports the hypothesis that O_3 arises from a reaction between $\text{O}(\text{}^3\text{P})$ and O_2 .⁸ As shown in Scheme 9, the reaction between $\text{O}^{\cdot-}$ and O_2 produces $\text{O}_3^{\cdot-}$. However, $\text{O}_3^{\cdot-}$ is rapidly protonated at neutral

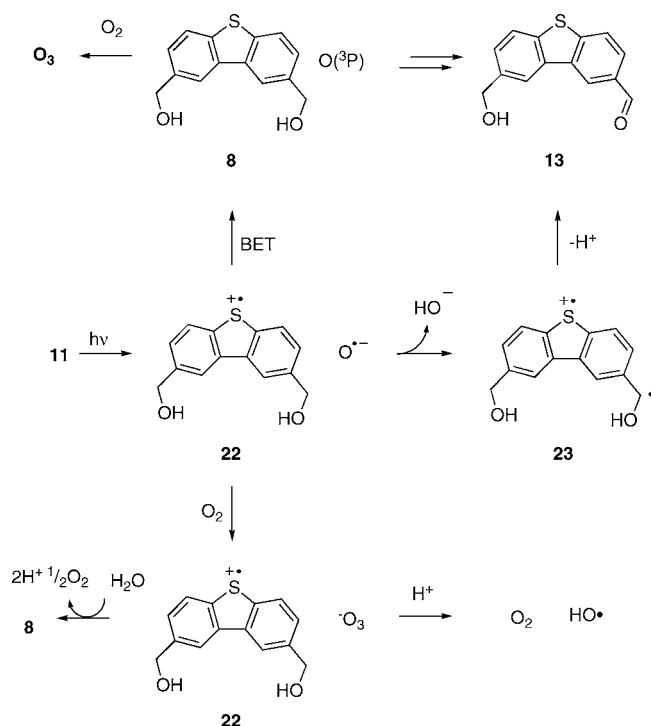
(35) Lee, J.; Grabowski, J. *Chem. Rev.* **1992**, 92 (7), 1611–1647.

(36) Ellis, H.; Poole, L. *Biochemistry* **1997**, 36 (48), 15013–15018.

(37) Xu, G. Z.; Chance, M. R. *Anal. Chem.* **2005**, 77 (8), 2437–2449.

(38) Bucher, G.; Scaiano, J. J. *Phys. Chem.* **1994**, 98 (48), 12471–12473.

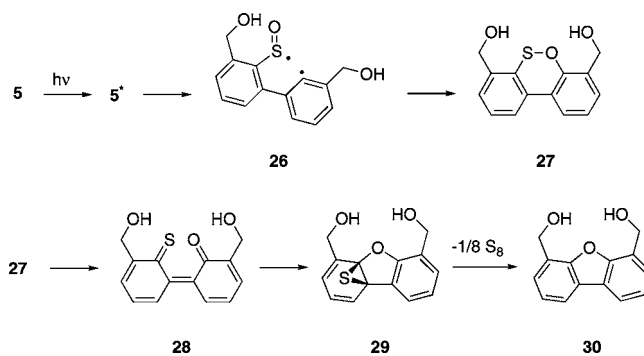
Scheme 9



pH to HO_3 , which decomposes back to $HO\cdot$ and O_2 .³⁹ Control experiments showed that **18** was not converted to **19** by $HO\cdot$, and thus, the oxidative cleavage of **18** does not likely involve discrete $O^{\cdot-}$.

A salient difference between the photochemistry of sulfoxides **5** and **11** was that an additional minor product was observed only during the photolysis of **5**. In negative-ion mode, ESI-MS revealed the unknown minor product specific to **5** gave rise to a $m/z = 259$ ($M - 1$) ion. This indicates the unidentified minor product arose from a unimolecular rearrangement of **5**. Photolysis of substituted thiophene S-oxides has been shown to yield the corresponding furans and sulfides as products.^{40–42} The furan products were thought to arise from photoinduced S–C homolysis followed by ring expansion to give a 1,2-oxathiine intermediate. Isomerization of 1,2-oxathiine followed by electrocyclization was postulated to yield an episulfide, which was thermodynamically driven to lose elemental sulfur to generate the observed furans. Thus, the dibenzo[*c,e*]oxathiine (**27**) could potentially be the observed unknown photoproduct of **5** as shown in Scheme 10. While the ring expansion has not been previously observed for dibenzothiophene S-oxides, the photoinduced ring-expansion has been observed for dibenzoselenophene *Se*-oxide.³ The isomerization **27** and subsequent electrocyclization to the episulfide **29** would be disfavored by the loss of aromaticity, which would explain why furan **30** was not detected. A possible explanation for why sulfoxide **5** and not sulfoxide **11** undergoes isomerization could be related to the location of the substituents. Increased torsional strain for the 4,6-substituted DBTO (**5**) could

Scheme 10



hinder the recombination of the biradical **26** and, thus, provide extra impetus for the ring expansion to **27**. However, since the assignment of the unknown product as **27** is speculative, additional evidence would be needed to confirm this hypothesis.

IV. Conclusions

The quantum yields for the photodeoxygenation of sulfoxide **5** and **11** increased in aqueous media. Analysis of the photo-products indicates that at least two different mechanisms can lead to the photoreduction of **5** and **11** in aqueous media. At high pH, photoinduced electron transfer leading eventually to a hydroxysulfuranyl radical that decomposes by heterolytic cleavage of the S–OH bond appears dominant. However, how this process leads to the oxidation of hydroxymethyl substituents remains unclear. In neutral and acidic conditions, the deoxygenation mechanism appears unimolecular, and the oxidative cleavage of alkenes strongly suggests $O(^3P)$ is formed to some extent. The increase in the photodeoxygenation quantum yields in water indicates the S–O bond scission is accompanied by charge separation, and thus, $O(^3P)$ is likely formed by back electron transfer from $O^{\cdot-}$ to a sulfide radical cation. It is unclear if discrete $O^{\cdot-}$ is formed; however, the increase in overall quantum yields and $\Phi_{+sulfoxide}/\Phi_{+formylsulfoxide}$ at low pH indicates protonation of $O^{\cdot-}$ could become significant as the pH of the solution decreases.

V. Experimental Section

Materials. Commercial materials were obtained from Aldrich or Fisher and used without modification, except as noted. Compounds **2–6**, **8–11**, and **15** were all prepared from modifications of known procedures that are described in the Supporting Information. Water was purified with a Milli-Q system.

4,6-Diformyldibenzothiophene (1). Dibenzothiophene (2.0 g, 10.8 mmol) and TMEDA (5.0 mL, 34.4 mmol) were dissolved in hexanes (60 mL) under argon atmosphere. The solution was then cooled to 0 °C. This was followed by dropwise addition of *n*-BuLi (20.0 mmol, 1.6 M in hexanes). The reaction was refluxed at 70 °C for 15 min and then was cooled to 0 °C. Anhydrous DMF (8.5 mL, 110 mmol) was added over 10 min, and the solution was allowed to warm to room temperature. The mixture was poured onto crushed ice and stirred for 1 h. The mixture was vacuum filtered and dried, and the resulting solid was recrystallized from toluene to afford **1** (2.0 g, 79%) as a white solid. Data for **1**. 1H NMR (400 MHz, $CDCl_3$): δ 10.352 (s, 2H), 8.883 (dd, $J_1 = 8.0$ Hz, $J_2 = 0.8$ Hz, 2H), 8.840 (dd, $J_1 = 7.6$ Hz, $J_2 = 0.8$ Hz, 2H), 7.886 (t, $J = 7.6$ Hz, 2H). ^{13}C NMR (400 MHz, $DMSO-d_6$): δ 192.74, 138.32, 134.97, 134.44, 130.76, 127.90, 125.51. HRMS (FAB): m/z calcd for $C_{14}H_8O_2S$ 240.024, found 240.024 IR (ATR): ν_{max} 1681, 1558, 1462, 1427, 1384, 1219, 1134, 995 cm^{-1} .

2,8-Diformyldibenzothiophene (7). 2,8-Dibromodibenzothiophene **6** (1.48 g, 4.3 mmol) was dissolved in dry THF (35

(39) Buhler, R. E.; Staehelin, J.; Hoigne, J. *J. Phys. Chem.* **1984**, *88* (12), 2560–2564.

(40) Nakayama, J.; Hiraiwa, S.; Fujihara, T. *J. Sulfur Chem.* **2008**, *29* (3–4), 243–250.

(41) Arima, K.; Ohira, D.; Watanabe, M.; Miura, A.; Mataka, S.; Thiemann, T.; Valcarcel, J.; Walton, D. *Photochem. Photobiol. Sci.* **2005**, *4* (10), 808–816.

(42) Heying, M. J.; Nag, M.; Jenks, W. S. *J. Phys. Org. Chem.* **2008**, *21* (11), 915–924.

mL) under argon atmosphere at $-78\text{ }^{\circ}\text{C}$. To this solution was added TMEDA (9.46 mmol), followed by dropwise addition of *n*-BuLi (10.75 mmol, 1.6 M solution in hexanes). The reaction was allowed to stir for 1 h. Anhydrous DMF (3.4 mL, 43.9 mmol) was added dropwise over 10 min, and the reaction was stirred for 3 h. The mixture was then poured into water and extracted with dichloromethane. The organic solution was dried with MgSO_4 and solvent removed under vacuum. The crude solid was purified by column chromatography (6:4 hexane/ethyl acetate) to yield 0.78 g (75%) of a white solid. Data for **7**. ^1H NMR (400 MHz, CDCl_3): δ 10.212 (s, 2H), 8.760 (s, 2H), 8.058 (m, 4H). ^{13}C NMR (400 MHz, $\text{DMSO-}d_6$): δ 192.43, 145.34, 134.91, 133.68, 127.03, 124.87, 124.07. HRMS (FAB): m/z calcd for $\text{C}_{14}\text{H}_8\text{O}_2\text{S}$ 240.024, found 240.024. IR (ATR): ν_{max} 1685, 1585, 1551, 1458, 1307, 1230, 1192, 810 cm^{-1} .

General Methods. NMR spectra were obtained using a Bruker DRX-400. High-resolution mass spectra were acquired using a JEOL JMS-700 MS. Photoluminescence spectra were obtained in EPA (5:5:2 methylbutane, ether, ethanol) at 77 K using a Photon Technology International modular fluorimeter. A Hewlett-Packard 1100 Series HPLC fitted with a quaternary pump and a diode detector array was used for all chromatographs on a 250 mm/4.6 μm Nucleosil 100-5 CN column. LCMS analyses were done on a Single Quad LCMS-2010EV with APCI or ESI modes using a C18 column for separations. A Shimadzu GCMS QP2010S using a DB-5 column for separations was used for GCMS analysis. The photolysis reactions were carried out in buffered and unbuffered solutions. For buffered solutions, a 0.1 M sodium acetate buffer pH 3.6 or a 0.1 M sodium glycine buffer pH 10.6 was used. Otherwise, the initial pH of the solutions was adjusted by adding either 0.1 M H_2SO_4 or 0.1 M NaOH until the desired pH was obtained. All pH measurements were made through the use of a Mettler Toledo pH meter.

Octanol–Water Coefficients. Octanol–water partition coefficients (K_{ow}) were determined experimentally using the shake-flask method. A solution of 8-octanol (5 mL) and water (5 mL) were allowed to come to a saturation equilibrium overnight. Approximately, 2–3 mmol of the desired compound was added to the solution in a capped test tube. The solution was continuously inverted over the period of 1 h and then centrifuged to eliminate emulsion. The octanol and water layers were then separated, and concentration of compound in each layer was assessed by HPLC.

Irradiations. For photolysis reactions run to complete conversion, solutions in fused-silica test tubes were irradiated in a Luzchem LZC-4C photoreactor using broadly emitting fluorescent bulbs centered at 350 nm. All samples were sparged with argon or oxygen prior to irradiation, and a few samples were degassed by five freeze–pump–thaw cycles. The progress of the reactions was monitored by HPLC. Most products were identified by comparison to authentic samples. Both 4-formyl-6-hydroxymethylidibenzothiophene (**12**) and 2-formyl-8-hydroxymethylidibenzothiophene (**13**) were extracted with 100 mL of CH_2Cl_2 from a basic photolysis mixture. The products were then isolated by preparative TLC using 2:3 hexane/ethyl acetate (**12**, $R_f = 0.50$; **13**, $R_f = 0.69$). The compounds were characterized as described in the text.

For irradiations at 254, 294, and 330 nm, a 75 W Xe lamp focused directly on a monochromator (Photon Technologies International) was used in most experiments. Slit widths were set to allow ± 6 nm linear dispersion from the given wavelength. Samples of 4.0 mL in 1 cm square optical cells were put in a permanently mounted cell holder where all exiting light hits the sample cell without further focusing. All samples were either sparged with argon or oxygen (>15 min) prior to photolysis. All

quantum yield experiments were carried out at a concentration high enough to reach an optical density >2 at the given wavelength and carried out to low conversion (<25%). Analysis of the reaction mixtures at various time points was performed with an HPLC. Photolysis of azoxybenzene to yield the rearranged product, *o*-hydroxyazobenzene, was used as an actinometer.²⁶

At 343 nm, the extinction coefficients of 9-methylcarbazole and **11** are 3200 and 700 $\text{M}^{-1}\text{ cm}^{-1}$, respectively. To ensure >97% of light was absorbed by the carbazole, a 4 mL sample containing 10 mM 9-methylcarbazole and <1 mM **11** in methanol was irradiated using the 75 W Xe arc lamp with the slits set to allow 4 nm of total linear dispersion. Oxygen was removed from the samples by bubbling argon, and the photolysis was monitored by HPLC.

Singlet oxygen was generated by bubbling oxygen through solutions containing 0.13 mM of methylene blue prior to irradiation. Irradiations were carried out using fluorescent bulbs fitted with 530 nm highpass filters in the LZC-4C photoreactor.

A set of photolysis reactions of **5** or **11** was carried out in EPA (ether/pentane/alcohol = 5:5:2) at 77 K. The sample, in a quartz NMR tube, was argon purged and quick frozen by submerging in liquid nitrogen in a transparent Suprasil Dewar. While continuously frozen, a 25 μM **11** sample was irradiated with a hand-held, short-wave UV lamp for 1 h. The resulting luminescence spectrum was obtained before the sample was melted and subjected to HPLC analysis. In another set of experiments, saturated solutions containing either **5** or **11** were irradiated with broadly emitting light centered at 350 nm for 30 min. The samples were then melted and subjected to HPLC analysis to determine product composition.

Electrochemistry. A CH instruments electrochemical analyzer model 700A was used for electrochemical experiments. All electrochemical measurements were performed in a one-compartment cell. Cyclic voltammetry was performed using one scan with a scan rate of 0.05 V/s. Square wave voltammetry was performed in acetonitrile solutions containing 0.1 M tetrabutylammonium perchlorate (TBAP) as the supporting electrolyte, and all samples were sparged with argon to remove oxygen immediately before the electrochemical measurement. A platinum disk was used as the working electrode and platinum mesh served as the auxiliary electrode. The reference electrode was Ag wire. Potentiostatic electrolysis of **2**, **5**, **8**, and **11** was carried out in a supporting electrolyte solution of 0.1 M tetrabutylammonium bromide (TBAB) in water. Before electrolysis, the solutions were purged of oxygen by bubbling dry argon for 30 min. The flow was kept over the liquid surface in the cell to prevent dissolution of oxygen during electrolysis. Platinum was used for the counter and working electrode, and the reference electrode was SCE. For **2** and **8**, the potential versus SCE was set at 0.8 V, and for **5** and **11**, the potential vs SCE was set at -1.7 V. The TBAB and TBAP were stored over P_2O_5 in a desiccator before use.

Acknowledgment. We thank Saint Louis University and the donors of the American Chemical Society Petroleum Research Fund for financial support of this research. We thank Shelley Minter and Paul Jellis for many helpful discussions.

Supporting Information Available: Detailed synthetic descriptions and ^1H NMR, ^{13}C NMR, MS, IR, and UV spectra of the compounds used in this work. Selected electrochemical measurements are included as well. This material is available free of charge via the Internet at <http://pubs.acs.org>.

JA100147B